Microinjection to deliver protein and mRNA into zygotes of the cnidarian endosymbiosis model *Aiptasia* sp.

Madeline Bucher[#], Victor A. S. Jones[#], Elizabeth A. Hambleton, Annika Guse*

Affiliation

Centre for Organismal Studies (COS), Heidelberg University, Heidelberg 69120, Germany

Contact Information:

M.B.: madeline.bucher@cos.uni-heidelberg.de; tel +49 6221 546252

V.A.S.J.: victor.jones@cos.uni-heidelberg.de; tel +49 6221 546252

E.A.H.: liz.hambleton@cos.uni-heidelberg.de; tel +49 6221 546264

[#]contributed equally

*corresponding author A.G.: annika.guse@cos.uni-heidelberg.de; tel +49 6221 546264

Key words

Aiptasia, Endosymbiosis, Emerging Model, *In Vitro* Fertilization, Microinjection, Functional Tools, Transgenesis

Abstract

Reef-building corals depend on an intracellular symbiosis with photosynthetic dinoflagellates for their survival in nutrient-poor oceans. Symbionts are phagocytosed by coral larvae from the environment and transfer essential nutrients to their hosts. *Aiptasia*, a small tropical marine sea anemone, is emerging as tractable model system for coral symbiosis; however, to date functional tools and genetic transformation are lacking. Here we have established an efficient workflow to collect *Aiptasia* eggs for *in vitro* fertilization and controlled microinjection as the basis for experimental manipulations in the developing embryo and larvae. We demonstrate that protein and mRNA can successfully be injected into live *Aiptasia* zygotes to label filamentous actin to mark cell outlines via recombinant Lifeact-GFP and cell membranes and nuclei via farnesylated mCherry and NLS-eGFP, in embryos and larvae. These proof-of-concept approaches pave the way for future functional studies of development and symbiosis establishment in *Aiptasia*, a powerful model to unravel the molecular mechanisms underlying intracellular coral-algal symbiosis.

Introduction

A complex yet fundamental puzzle in cell and developmental biology is how cells from different phyla coexist and co-function in symbiosis – how do very different cells encounter each other, what molecular conversations occur to promote symbiosis establishment, and how is such a complex partnership maintained in the steady state? An ecologically crucial symbiosis is that between reef-building corals and their single-celled dinoflagellate algae symbionts, which provide photosynthetically derived nutrients underlying the productivity and health of coral reef ecosystems (Muscatine, 1990; Yellowlees, 2011). Strikingly, most corals must re-establish this vital symbiosis anew every generation in the larval or juvenile stage by taking up algal cells from the environment into the gastric cavity, after which they are phagocytosed into endodermal cells and reside as endosymbionts inside a specialized organelle, the symbiosome (van Oppen et al., 2001; Wakefield and Kempf, 2001; Rodriguez-Lanetty et al., 2009; Harii et al., 2009). Despite its importance, we know little regarding the molecular basis of the establishment of coral-algal symbiosis during development.

We are only slowly making progress towards a better understanding of symbiosis establishment, primarily due to the historical lack of tools and workable laboratory systems: until very recently, neither the target organisms nor other related laboratory models have been suitable. Reef-building corals are poor laboratory subjects as they grow slowly, are sensitive to environmental conditions, and typically produce sexual offspring in the form of planktonic larvae only once annually (Babcock, et al., 1986; Technau and Steele, 2011; Harrison, 2011). Likewise, most other current cnidarian laboratory models such as Hydra, *Nematostella*, *Clytia*, and *Hydractinia* are not symbiotic (the exception, *Hydra viridissima*, hosts symbionts unrelated to those in corals and lacks a free-swimming larval stage). The advent of modern molecular tools has made establishing new model systems far more feasible, and we and our colleagues have developed the small marine anemone *Aiptasia* into a powerful model for molecular studies of coral-algal symbiosis (summarized in Weis et al., 2008; Goldstein and King, 2016). Housing the same symbionts as corals yet tractable in the laboratory, *Aiptasia* now has a range of key resources including a sequenced genome, transcriptomes of many states (e.g. symbiotic *vs.* non-symbiotic), advanced microscopy, phenotypic assays, and controlled regular production of offspring in the laboratory (Sunagawa et al., 2009; Lehnert et al., 2014; Xiang et al., 2014; Baumgarten et al., 2015; Bucher et al., 2016; Grawunder et al.,

2016). Just as in corals, *Aiptasia* larvae phagocytose symbionts from the environment (Hambleton et al., 2014; Wolfowicz et al., 2016).

Despite its success, *Aiptasia* has so far lacked tools important for a cell and developmental model system: namely, the introduction of exogenous material or the perturbation of endogenous processes. Such ability would be especially useful to study how *Aiptasia*, and by extension reef-building corals, establish symbiosis anew in the developing larval stage. To this end, microinjection of material into embryos has proven an efficient method of accomplishing genetic engineering in many models, while also making possible the direct production of F0 manipulated larvae and juveniles for immediate phenotypic analysis.

There are currently no published reports of microinjection in *Aiptasia* nor any symbiotic cnidarian, with one exception of an elegant study involving the injection of morpholinos into recently spawned coral embryos (Yasuoka et al., 2016). While an important step forward, the aforementioned difficulties of efficient laboratory work in corals means that a more fruitful long-term approach would be developing these techniques in the *Aiptasia* model. We have excellent guides not only from the referenced coral study but also from the use of such tools in the cnidarian models *Hydra*, *Nematostella*, *Clytia*, and *Hydractinia*, in all of which successful microinjection and genetic engineering protocols are employed (Momose et al., 2007; Wittlieb et al., 2006; Renfer et al, 2009; Kunzel et al., 2010; Marlow et al., 2012; Layden et al., 2013, Ikmi et al., 2015; Artigas et al., 2017).

The development of microinjection and the subsequent introduction of foreign material would be ground-breaking for the *Aiptasia* and coral-algal symbiosis fields. It would open the door to myriad observational and functional studies, propelling the symbiosis field forward and allowing both broad approaches as well as specific hypothesis testing based on candidate genes. To this end, here we show the establishment of microinjection in the *Aiptasia* model system in a clear and consistent workflow to introduce exogenous material into embryos for subsequent analysis. We describe conditions for regular gamete production as a prerequisite to efficient microinjection. We then show successful introduction of two key materials: fluorescent protein and mRNA, with direct visualization of the protein (recombinant Lifeact-eGFP protein) or its protein products (mRNA encoding nuclear-directed eGFP and membrane-bound mCherry). Most importantly, we show that such exogenous material introduction appears to have no significant effects on either development or

symbiosis establishment in the manipulated larvae, demonstrating the utility of these tools to study fundamental questions of development and symbiosis establishment in the *Aiptasia* system.

Results

Optimized spawning system and *in vitro* fertilization for zygote production

An important prerequisite for the effective delivery of molecules to sufficient numbers of eggs and developing zygotes via microinjection is control over fertilization, which would allow regular access to developmentally synchronized stages for microinjection. We previously established a robust and consistent protocol for spawning induction of *Aiptasia* in the laboratory based on a blue light cue (simulated full moon) (Grawunder et al., 2015). Building on this, here we optimized a controlled anemone cultivation system to induce spawning in female and male anemones separately for collection of gametes and *in vitro* fertilization. Staged sets of mature adult anemones were grown individually in small tanks and induced to spawn with the monthly blue light cue. Tanks were monitored for two consecutive months (two lunar simulations); the second month of an old set of tanks overlapped with the first month of a new tank set, so that there was always one set of tanks in its first month and one in its second. Spawning was checked every day of the work week (Mon-Fri) from 9 am-10 am, approx. 5-6 h after the onset of darkness (12L:12D photoperiod with darkness from 4 am – 4 pm). Spawning typically occurred during the third and fourth weeks after the start of the blue light cue (Fig. 1A). Gametes were produced on average 2.7 times per week (n=24 weeks), and microinjection was therefore possible on most Wednesdays, Thursdays, and Fridays (Fig. 1B). After spawning, eggs were often found in a discrete patch on the tank bottom near the female (Fig. 1C). Sperm was sometimes observed either as an obvious expelled cloud or as milky tank water, yet even when they were too dilute to be detected via stereoscope, they were nevertheless often present (confirmed with DIC microscopy and/or staining of sperm nuclei with Hoechst [data not shown]).

We next mixed spawned gametes and assessed the efficiency of *in vitro* fertilization. Several hundred eggs from a discrete patch were gently aspirated using a plastic transfer pipette and transferred into a small plastic petri dish, into which sperm-containing water was then added. Fertilization efficiency was quantified after approximately 4-5 h, at which point developing zygotes could be clearly distinguished

from unfertilized eggs. We found that on average, only 20% of eggs were fertilized in uncoated petri dishes; however, using dishes that were pre-coated with 0.1% gelatin in distilled water yielded mean fertilization rates of 87% (Fig. 1D). Coating dishes with 1% BSA in distilled water or agarose in filtered artificial seawater (FASW) was equally effective (data not shown). We noted that it was important to add sperm to the eggs as soon as possible after spawning. On average, while more than 90% of eggs were fertilized when sperm was added within 15 min after egg release, fertilization rates fell rapidly over time, reaching 20% when sperm was added to eggs 60 min post-spawning and nearly 0% after 120 min (Fig. 1E). Thus, time is of the essence to ensure high fertilization rates.

Establishment of an efficient *Aiptasia* zygote microinjection procedure

Mixed gametes were left for approx. 10 min to allow *in vitro* fertilization, during which time the microinjection apparatus was prepared. Following Wessel et al., 2010, the injection dish was prepared ahead of time by affixing a strip of nylon mesh (80 x 80 µm) to the lower inside surface of a small petri dish lid, using a line of silicon grease around the edges of the mesh (Fig. 2A). FASW was then added to cover the bottom entirely, and zygotes were added in a line above the mesh strip, spread relatively sparsely to facilitate later retrieval. We noted that zygotes as well as developing embryos are sensitive and should be pipetted as gently as possible to avoid developmental defects. As *Aiptasia* zygotes are approx. 86 µm in diameter (Bucher et al., 2016), they settle into the holes of the mesh but do not fall through (Fig. 2B). We injected using a stereoscope keeping the dish stationary and moving the needle between zygotes and along its own axis to enter each zygote (Fig. 2C). Zygotes were injected such that the injected material occupied approx. a third to half of the cell diameter corresponding to approximately 10% of the egg volume, as assessed visually by the tracer dye or fluorescent protein. In both these cases the fluorescence persisted long after injection and was used to distinguish injected from non-injected zygotes (Fig. 2D).

In order for the injected molecules to reach all cells, microinjection must occur before the first cell division and cytokinesis is complete. Typically, the first clearly visible indication of development in *Aiptasia* zygotes is the appearance of 4-cell stages ~90 min after fertilization (asterisk, Fig. 2D). We observed that zygotes appear slightly box-shaped (Fig. 2E) shortly before membrane invagination and cleavage occurs, and at this point we ceased injecting. Occassionally, we observed two discrete nuclei before the first obvious cleavage, likely indicating that the first nuclear division

happens without cytokinesis. The next cleavage to form 8 cells occurs ~20 min later after the first, and embryonic development continues until the blastula stage is reached approximately 5 hours post-fertilization (hpf), at which point successfully-developing embryos could be easily distinguished from unfertilized eggs (arrowhead, Fig. 2F). Using this system, with practice, one person can inject more than 100 zygotes in the roughly 1 h window before the first cell divisions begin.

We quantified the survival rates after 24 h of injected embryos versus those handled exactly the same way but not injected. Embryos injected with any of a variety of material (i.e. protein and mRNA; see below) had a survival rate of approx. 49% (332 of 677 injected embryos). In comparision, the survival rate of control embryos was approx. 61% (306 of 501 control embryos), which did not differ significantly from that of the injected set (Student's 2-tailed unpaired t-test, p-value =0.24).

Microinjection of fluorescent protein into *Aiptasia* larvae

To visualize cell outlines in the developing larvae, we recombinantly expressed and purified Lifeact-eGFP protein (Fig. 3A), which in other systems labels the actin cytoskeleton and has little to no effect on live actin cellular dynamics (Riedl et al., 2008; Sliogeryte et al., 2016). Microinjected protein instantly and ubiquitously labeled cell outlines in *Aiptasia* zygotes throughout the first cell divisions and through to larvae 24h post-injection, especially in the ectodermal tissue (Fig. 3B). Prominent but weaker staining was still visible 48h after injection, but staining intensity decreased with larval age and was basically undetectable 4 days after injection. Importantly, we did not notice any appreciable defects or delays in development in injected embryos relative to uninjected controls (data not shown).

Microinjection and *in vivo* translation of exogenous mRNA in *Aiptasia* larvae

To visualize cell outlines on a longer timescale, as well as to test whether exogenous mRNA is efficiently translated in *Aiptasia* zygotes, we next injected *in vitro* transcribed bicistronic mRNA from a plasmid encoding eGFP with a nuclear localization signal (NLS-eGFP) and mCherry with a farnesylation signal (mCherry-CaaX) separated by the self-cleaving V2A peptide (Fig. 4A). mRNA from this construct was previously shown to simultaneously label cell membranes and nuclei in developing embryos of the anemone *Nematostella* (Ikmi et al., 2014). Injected mRNA was translated robustly as indicated by a strong, homogeneous and long-lasting fluorescent labeling of the cellular structures (Fig. 4B). Labeled membranes and nuclei were detected as early as 4 hpf. At 6 hpf (blastula stage), signal intensity had

further increased, with intensely labeled nuclei and membranes that remained so for 1-2 days post-fertilization (dpf). Fluorescent labeling of cell membranes and nuclei persisted on a longer timescale than the injected Lifeact-eGFP protein; signal was detectable 10 dpf, with the nuclei still very intensely labeled but the membranes much dimmer (possibly due to high membrane turnover) (Fig. 4B).

Symbiosis establishment in mRNA-injected larvae

Importantly for the applicability of this technique to the study of symbiosis, mRNA injection did not appear to affect symbiont uptake by *Aiptasia* larvae. Using our standard symbiosis establishment assay (Bucher et al., 2016), we exposed injected and control larvae to a compatible symbiont strain and analyzed symbiosis establishment. Injected larvae appeared developmentally normal and took up symbionts from the environment; imaging by confocal microscopy showed phagocytosed algae within the host endodermal tissue that could be clearly distinguished from those in the gastric cavity (Fig. 4C). In four experiments, each with matched injected and control larvae, infection rates did not differ significantly between mRNA-injected larvae (47%) and non-injected control larvae (66%) (Student's 2-tailed unpaired *t*-test, *p*-value = 0.14). Likewise, the average number of algal cells that each infected larvae contained was similar (injected larvae 3.8 algae/larva, uninjected control larvae 3.7 algae/larvae; Student's 2-tailed unpaired *t*-test, *p*-value = 0.37).

Discussion

Here we establish a workflow to successfully introduce exogenous protein and mRNA via microinjection into *Aiptasia* zygotes and, critically, we demonstrate that such manipulation has no significant effects on development or symbiosis establishment in *Aiptasia* larvae. This progress propels the *Aiptasia* model system forward in answering fundamental questions regarding development and concurrent establishment of coral-algal symbiosis. While immediately permitting a range of observational and functional assays, it also opens the door to CRISPR-Cas9-induced gene editing and the production of stable transgenic lines. Finally, this work holds broader implications for comparative developmental biology and emerging technologies in the current bloom of new model systems across the life sciences.

This workflow immediately permits in the *Aiptasia* larval system many observational and functional assays that bring us closer to understanding larval development and symbiosis establishment. The small transparent larvae of *Aiptasia* are amenable to microscopy, which we have until now used to assay fixed specimens (Hambleton et al., 2014; Bucher et al., 2016). Thus, the investigation of development and the symbiosis establishment process was necessarily limited to “snapshots”; now, the live imaging of symbiosis dynamics becomes possible. Further, commercially available dyes can be (co)injected to (co)label other conserved cellular structures.

To study developmental processes, larvae with labeled cell outlines (Figs 3, 4) and live imaging can be used to characterize developmental processes such as gastrulation, tissue differentiation, and cell division and migration. Injected recombinant Lifeact-eGFP protein instantly labels all cells in developing zygotes and may serve as the basis to analyze the dynamics and cellular details of *Aiptasia* embryonic development. Similarly, injection of *NLS-eGFP-V2A-mCherry-CaaX* mRNA allows monitoring of the dynamics of cellular and nuclear behavior once translation has started. Early and homogenous expression of exogenous mRNA also allows the manipulation of developmental genes, such as those involved in patterning and axis establishment, to monitor dynamics or create overexpression phenotypes.

To study symbiosis establishment in *Aiptasia* larvae, key goals are to test candidates for their roles in symbiosis as well as to observe over time when and where in the larval endoderm symbionts are phagocytosed and how they subsequently proliferate throughout the tissue. Importantly, we can immediately tackle the first goal by using injected mRNA. We envision, for instance, that one could express proteins fused to fluorescent tags to track their co-localization with symbionts or interactions with other proteins, or analyze the effects of the over-expression phenotypes of symbiosis-specific genes on symbiosis establishment. The constructs reported here have proven limited for observing symbiont phagocytosis and proliferation with cellular resolution; both the directly injected LifeAct-eGFP protein and exogenously expressed farnesylated mCherry mark cell outlines, but lose resolution in the endoderm in older larvae (Figs 3,4). This phenomenon has also been reported in *Nematostella*, where signal from some mRNA lasts for up to two months after injection, but others are rapidly lost (DuBuc et al., 2014). There is however overlap between signal and symbiosis, as *Aiptasia* larvae acquire symbionts at and after 2 dpf, and signal of the mRNA fades several days later. Nevertheless, these particular

tools may be modified to attempt to boost signal duration; alternatively, they may never be optimal for this application, but could still be used as a launching point to develop more appropriate tools, such as stable transgenic lines. A current obstacle to this is that metamorphosis and settlement of larvae into adults cannot yet be accomplished in the laboratory; multiple groups are actively working towards identifying the cue to induce closure of the life cycle.

The *Aiptasia* field, and by extension the coral-algal symbiosis field, acutely requires tools to translate knowledge on molecular players into a mechanistic understanding at the functional level. In addition to the gain-of-function possibilities outlined above, the ability to deliver materials by microinjection facilitates the next major leap forward for the *Aiptasia* model: gene editing by CRISPR-Cas9. Such gene editing would allow, for the first time, knock-out of candidate genes implicated in symbiosis establishment to unequivocally and functionally demonstrate their role in symbiosis. Likewise, tagging of genes by, for example, insertion of N- or C-terminal fluorophores into endogenous loci, would allow visualization of their dynamics during symbiosis establishment. Further, replacing genes with others allows more unusual types of experiments, e.g. probing of gene function and the extent of gene conservation between species. It is apparent that when developing a new model, not all techniques can be established and not all questions can be addressed at once. Although the use of microinjected constructs or CRISPR-Cas9 to create stably altered lines must await the closure of the *Aiptasia* life cycle in the laboratory, the techniques can, crucially, be employed immediately for urgent questions. Here we show that *Aiptasia* zygotes can be injected in sufficient numbers and the larvae used for symbiosis studies in the F0 generation (i.e. the injected animals themselves).

Beyond the *Aiptasia* system, this work holds broader implications for comparative developmental biology and other emerging model systems. The studies of embryonic development in *Aiptasia* discussed above would complement those in other systems to dissect the evolution of fundamental developmental processes, such as gastrulation. As the sister group to bilaterians, cnidarians are important “EvoDevo” models to infer evolutionary conservation and divergence of development reviewed, for example, in Layden et al. (2016) and Technau and Steele (2011).

The advent of modern research tools has led to rapid advances in emerging models, as new avenues are opened to study previously intractable cell biological questions (Cook et al., 2015; Goldstein and King, 2016). For example, low-cost next-generation

sequencing allows genomes and transcriptomes to be quickly sequenced and analyzed, providing the framework for molecular analysis for any given process of interest. The abundance of commercially available molecular dyes and cytoskeletal probes allows live imaging of dynamic changes in cell behavior and organization during development and disease in basically any given system. CRISPR-Cas9-induced gene editing is likewise an affordable and widely applicable method to tag or disrupt genes of interest in virtually any living organism to specifically probe the function of key molecules. The *Aiptasia* system is currently undergoing this transition: a wealth of resources has been recently and rapidly built, but missing was the transformative power of manipulation via introduction of exogenous material or targeted functional analysis. Our progress on this front was of course inspired by successful techniques in other model systems, and we hope this work in turn provides helpful "lessons learned" for other emerging models. For example, optimized spawning, *in vitro* fertilization, and an efficient microinjection configuration are all crucial in allowing sufficient numbers of injected larvae for analysis, and these techniques are likely applicable to other species. With the rapid development of myriad new model systems, we are in the midst of an exciting time for major discoveries in underexplored cell biological phenomena.

Author contributions

M.B., V.A.S.J., E.A.H. and A.G. designed the experiments. M.B. and V.A.S.J. performed the experiments. M.B., V.A.S.J., E.A.H. and A.G. wrote the manuscript. All authors reviewed and approved the manuscript.

Acknowledgments

Funding was provided to A.G. by the Emmy-Noether-Programme of the German Research Foundation (DFG) (grant no. GU 1128/3-1), by a Marie Curie Career Integration Grant (CIG) under the FP7-PEOPLE-2013-CIG program, European Commission, and by an ERC Consolidator grant (project ID 724715); and to V.A.S.J. by an EMBO Long-Term Fellowship. We thank Natascha Bechtoldt for technical help, and Steffen Lemke, Thomas Holstein, Suat Özbek, Jochen Wittbrodt and Aissam Ikmi, for advice, comments, and sharing reagents and equipment. We also thank

Christian Ackermann at the Heidelberg Nikon Imaging Center for technical support with microscopy.

Material and Methods

Anemone cultivation for spawning induction

Individuals to be used for gamete production were produced asexually by pedal laceration from adult animals in master stock tanks of either male CC7 (Sunagawa et al., 2009) or female F003 (Grawunder et al., 2015) clonal lines. To raise them to sexual maturity, 12-14 medium-sized animals of each line (with an oral disc diameter of 4-5 mm for F003 and 5-6 mm for CC7) were maintained for 6-7 months as previously described (Grawunder et al., 2015), in covered, food-grade plastic tanks in a volume of approximately 1.6 l artificial sea water (ASW). Briefly, tanks were kept at 26°C with a 12L:12D photoperiod from 8 am to 8 pm to allow observation and maintenance during the daytime. Animals were fed five times a week with fresh *Artemia* nauplii. Three times per week, the surfaces of the tanks were cleaned with cotton swabs and ASW was exchanged. During this period anemones of both lines grew to reach an oral disc diameter of 11-12 mm.

Spawning induction and *in vitro* fertilization of *Aiptasia*

To prepare sexually segregated tanks of *Aiptasia* for gamete release, 3-5 mature animals of either CC7 or F003 were transferred into 300 ml ASW in smaller tanks (Cat. Num. 92CW, Cambro, USA) one week before spawning induction to allow acclimatization to the new tank. Tanks were fed and cleaned as described above. Tanks were then kept at 29°C in Aqualytic Incubators (Model TC 135 S, Liebherr, Germany) equipped with white LEDs (SolarStinger Sunstrip “Marine”, Cat. Num. 00010446, Econlux, Germany) at an intensity of 23-30 µmol m^{-2} s^{-1} on a 12L:12D photoperiod with darkness from 4 pm to 4 am, thereby adjusting the animals’ diurnal rhythms to allow gamete collection during working hours. To induce gamete release following a simulated full moon cue, animals were exposed to blue light LEDs (SolarStinger Sunstrip “Deepblue”, Cat. Num. 00010447, Econlux, Germany) at 15-20 µmol m^{-2} s^{-1} for the entire dark phase on days 1 to 5 of a 28-day cycle (Grawunder et al., 2015).

Tanks were examined for the presence of eggs or sperm using a Leica S8APO stereoscope between days 13 and 24 of each cycle from 9 am-10 am (i.e. 5-6 h after

onset of darkness). Eggs from F003 (female-only) tanks were transferred gently with a plastic transfer pipette into a small plastic petri dish (60 mm x 15 mm) in a volume of approx. 5-10 ml. On occasion, spawned eggs float instead of forming discrete patches; we had previously tried to concentrate these using small 40 µm filters, but the handling substantially reduced the number of normally developing embryos. We therefore used only spawning events that resulted in egg patches for microinjection (Fig. 1C). To fertilize the eggs, approx. 3-7 ml water from several CC7 (male-only) tanks was added to dish to maximize the chances of sperm presence and fertilization.

Noticing low fertilization rates in preliminary experiments, we compared *in vitro* fertilization efficiency of gametes mixed in uncoated petri dishes to those in dishes pre-coated with gelatin. To coat, a 0.1% solution of gelatin in distilled water was poured into the dishes, incubated at room temperature (RT) for 5 min, removed, and then the dishes were air-dried at RT overnight and stored at RT until further use. Eggs were added to the dishes as described above, and sperm-containing water was then added at the indicated time-points in Fig. 1F. Based on the outcome of these comparisons (Figs 1E,F), eggs for microinjection were afterwards always prepared in a 0.1% gelatin-coated dish and mixed with water from CC7-containing tanks, as described above, as soon as possible after gamete release. The eggs and sperm were incubated together at RT for approx. 10 min to allow fertilization to occur while preparing the equipment and solutions for microinjection.

Expression of Lifeact-eGFP protein in bacteria

The Lifeact-eGFP sequence with a C-terminal 6His-tag was PCR amplified from the plasmid described by Riedl et al. (2008) and subsequently cloned into the pET21a vector using classical restriction-based cloning methods. For expression in *E.coli*, cells of strain BL21 were transformed with the plasmid via chemical transformation. A single colony of transformants was picked and grown in 1 l of LB medium to an OD_{600} of 0.6, at which time protein expression was induced by adding IPTG to a final concentration of 1 mM. Bacterial cells were recovered by centrifugation at 2,070 *xg* for 20 min, washed with 50 ml PBS, and re-centrifuged exactly as above. The pellet was then frozen in liquid nitrogen, stored at -80°C, and quick-thawed at 37°C the following day. 40 ml lysis buffer (50 mM $NaPO_4$ pH 8.0, 0.5 M NaCl, 0.5% glycerol, 0.5% Tween-20, 10 mM imidazole, 1 mg/ml lysozyme) was added onto each pellet and pipetted up and down several times in order to lyse bacterial cells. After stirring for 15 min at 4°C, the lysate was sonicated on ice with several 15-30 s pulses until

no longer viscous. To clarify the lysate, it was spun at 37,059 *xg* for 1 h at 4°C. The supernatant was then mixed with 2 ml pre-washed Ni-NTA agarose beads (Cat. Num. 31105, Cube Biotech, Germany) and protein allowed to bind to the beads by rotating 2 h at 4°C. Beads with bound protein were washed with three times with 20 ml wash buffer 1 (50 mM $NaPO_4$ pH 8.0, 250 mM NaCl, 0.05% Tween-20, 20 mM imidazole), once with 20 ml wash buffer 2 (50 mM $NaPO_4$ pH 6.0, 250 mM NaCl, 0.05% Tween-20, 20 mM imidazole) and twice 20 ml modified wash buffer 1 (50 mM $NaPO_4$ pH 8.0, 250 mM NaCl, 20 mM imidazole). Between each wash, beads were pelleted by centrifuging for 3 min at 2,800 *xg* at 4°C. Beads were carefully transferred into a poly-prep chromatography column (Cat. Num. 7311550, BioRad Laboratories) and the protein was eluted with sequential applications of 500 µl elution buffer (50 mM $NaPO_4$ pH 8.0, 150 mM NaCl, 250 mM imidazole, 5% glycerol). Collected protein fractions were analyzed using SDS-PAGE. Fractions with the highest protein content were pooled and dialyzed against 1x PBS. Protein concentration was determined via Bradford assay and absorbance measurements at A280 using a Nanodrop 1000 (Thermo Scientific). Protein aliquots were flash-frozen in liquid nitrogen and stored at -80°C until further use.

Synthesis of mRNA for microinjection

The *NLS-eGFP-V2A-mCherry-CaaX* construct was transcribed from the pSYC-97 vector (Kim et al., 2011; Ikmi et al., 2014; a kind gift from Aissam Ikmi). mRNA was synthesized using the mMESSAGE mMachine SP6 kit (Thermo Fisher Scientific) and purified with the RNeasy Mini Kit (Qiagen), according to the instructions in both kits. The quality and concentration of the mRNA was assessed on a 1% agarose gel and with a Nanodrop 1000 (Thermo Fisher Scientific). The mRNA was then diluted to 600 ng/µl with RNase-free water and single-use aliquots of 2 µl each were stored at -80°C until use.

Microinjection

Microinjection was carried out in dishes made from the lids of small petri dishes (35 x 10 mm). A strip of 80 µm nylon mesh (Cat. Num. SW10080.010.010, Meerwassershop (www. Meerwassershop.de), Germany) was affixed to the base of the lid using silicon grease around the edges. Filtered ASW (FASW) was added to the dish until the entire base was covered. Zygotes were concentrated in the center of the fertilization dish by gentle rotation, and slowly taken up with a 10 µl pipette with a plastic disposable tip. The zygotes were gently ejected into the injection dish under water, so that they fell sparsely in a stripe onto the mesh and settled into the holes.

For Lifeact-eGFP protein, an aliquot was quick-thawed and injected at a concentration of ~3.4 mg/ml, using the green fluorescence of the protein itself as an injection tracer. For mRNA, an aliquot of 600 ng/µl was thawed and mixed 1:1 with 0.5% phenol red in RNAse-free water as an injection tracer, for a final concentration of 300 ng/µl mRNA. Phenol red, a pH indicator that appears yellow when intracellular but red in seawater, provides a clear indication of when injection has been successful and, crucially, does not interfere with later fluorescence. Its disadvantage is that it quickly dissipates from zygotes, requiring that they be transferred to a separate dish very soon after injection, interrupting the work. For optimization of injection methods or in cases where competing fluorescence is irrelevant, a fluorescent tracer is preferable because they remain in zygotes longer and facilitate later selection of injected zygotes; we have used 10,000 MW Dextran coupled to Alexa 594 dye (Fig. 2D) (Cat. Num. D22913, Invitrogen).

Injection solution was loaded into a Femtotip needle (Cat. Num. 5242952008, Eppendorf) using Microloader tips (Cat. Num. 5242956003, Eppendorf) and allowed to run into the tip by gravity flow. Microinjections were performed with a manual micromanipulator (U-31CF micromanipulator [Narishige, Japan] with a standard universal capillary holder [Cat. Num. 920007392, Eppendorf] and Femtotip adapter [Cat. Num. 5176190002, Eppendorf]) attached to a FemtoJet 4i microinjector (Cat. Num. Num. 5252000013, Eppendorf). The angle of the needle holder to the bench-top was approximately 55°. Either the “constant flow” or the “injection” setting on the microinjector was used to deliver the solution into the cell. Solution flow and approx. injected amount (roughly 1/3 cell diameter or approx. 10% of cell volume) was visually assessed during the session and the pressure adjusted as necessary; during the session, the needle tip may need to be broken to remove blockages and then the injection pressure recalibrated. Microinjections were conducted either on a Nikon SMZ18 stereoscope or a Leica MSV269 stereoscope using a 0.5x objective or 1x objective, respectively. Injection was conducted either under white illumination to visualize zygotes and phenol red tracer, or, when applicable, indirect white illumination together with additional epifluorescent illumination and filters to visualize protein/tracer fluorescence.

Zygotes were injected for approx. 60 min, corresponding to until approx. 90 min after fertilization, at which time the first cleavages began. Zygotes injected using the tracer phenol red were transferred immediately after injection (before the tracer disappeared) by aspirating them individually into the well of a 6-well culture plate

filled with approximately 5 ml of FASW using a P10 pipette. Zygotes injected with Lifeact-eGFP or other fluorescent tracer could be distinguished from non-injected zygotes and transferred at the end of the injection session. Eggs that were uninjected but otherwise handled identically in all steps, including addition to and removal from the injection dish, served as controls. Plates with microinjected embryos were kept in the dark at 29°C to develop.

Assay of symbiosis establishment in larvae

Infection of injected or control larvae with *Symbiodinium* strain SSB01 (Xiang et al., 2013) was performed as described previously (Bucher et al., 2016). Briefly, larvae were kept in 5 ml of FASW in a 6-well plate, and algae were added to a final concentration of 100,000 algal cells/ml and mixed gently with a pipette. Algae and larvae were co-cultivated for 3 days, after which larvae were fixed, mounted on slides, and assessed by epifluorescence microscopy, as described below. Infection rates were determined by counting the number of larvae containing algae (percent infected) and the number of algal cells that each infected larva contained, as described previously (Bucher et al., 2016).

Microscopy and image analysis

Transmitted light and fluorescence images of live zygotes in Fig. 2 were acquired using a Nikon SMZ18 binocular microscope. Larvae in Figs 3 and 4 were fixed at the indicated time-points in 3.7% formaldehyde in FASW for 30 min, washed three times in PBS-0.2% Triton X100, and mounted in 50% glycerol in PBS. Images in Figs 3 and 4 were acquired using a Nikon A1 confocal microscope with a Nikon Plan Fluor 60× water immersion objective and Nikon Elements Software. All image processing was performed using Fiji (Schindelin et al., 2012).

References

Artigas, G. Q., Lapébie, P., Leclère, L., Takeda, N., Deguchi, R., Jékely, G., Momose, T. & Houliston, E. (2017). CRISPR/Cas9 mutation of a gonad-expressed opsin prevents jellyfish light-induced spawning. bioRxiv doi: 10.1101/140210

Babcock, R. C., Bull, G. D., Harrison, P. L., Heyward, A. J., Oliver, J. K., Wallace, C. C.& Willis, B. L. (1986). Synchronous spawnings of 105 scleractinian coral species on the Great Barrier Reef. *Mar Biol* **90**, 379-94.

Baumgarten, S., Simakov, O., Esherick, L. Y., Liew, Y. J., Lehnert, E. M., Michell, C. T., Li, Y., Hambleton, E. A., Guse, A., Oates, M. E., *et al.* (2015). The genome of *Aiptasia*, a sea anemone model for coral symbiosis. *Proc Natl Acad Sci USA* **112**, 11893-8.

Bucher, M., Wolfowicz, I., Voss, P. A., Hambleton, E. A. & Guse, A. (2016). Development and symbiosis establishment in the cnidarian endosymbiosis model *Aiptasia* sp. *Sci Rep* **6**, 19867.

DuBuc, T. Q., Dattoli, A. A., Babonis, L. S., Salinas-Saavedra, M., Rottinger, E., Martindale, M. Q. & Postma, M. (2014). *In vivo* imaging of *Nematostella vectensis* embryogenesis and late development using fluorescent probes. *BMC Cell Biol* **15**, 44.

Goldstein, B. & King, N. (2016). The future of cell biology: Emerging model organisms. *Trends Cell Biol* **26**, 818-24.

Grawunder, D., Hambleton, E. A., Bucher, M., Wolfowicz, I., Bechtoldt, N. & Guse, A. (2015). Induction of gametogenesis in the cnidarian endosymbiosis model *Aiptasia* sp. *Sci Rep* **5**, 15677.

Hambleton, E. A., Guse, A. & Pringle, J. R. (2014). Similar specificities of symbiont uptake by adults and larvae in an anemone model system for coral biology. *J Exp Biol* **17**, 1613-9.

Harii, S., Yasuda, N., Rodriguez-Lanetty, M., Irie, T. & Hidaka, M. (2009). Onset of symbiosis and distribution patterns of symbiotic dinoflagellates in the larvae of scleractinian corals. *Mar Biol* **156**, 1203-12.

Harrison, P. L. Sexual reproduction of scleractinian corals. In *Coral Reefs: an Ecosystem in Transition* (*eds*. Zubinsky, Z. & Stambler, N.) 59-85 (Springer, 2011).

Ikmi, A., McKinney, S. A., Delventhal, K. M. & Gibson, M. C. (2014). TALEN and CRISPR/Cas9-mediated genome editing in the early-branching metazoan *Nematostella vectensis*. *Nat Commun* **5**, 5486.

Kim, J. H., Lee, S. R., Li, L. H., Park, H. J., Park, J. H., Lee, K. Y., Kim, M. K., Shin, B. A. & Choi, S. Y. (2011). High cleavage efficiency of a 2A peptide derived from porcine teschovirus-1 in human cell lines, zebrafish and mice. *PLoS One* **6**, e18556.

Künzel, T., Heiermann, R., Frank, U., Müller, W., Tilmann, W., Bause, M., Nonn, A., Helling, M., Schwarz, R. S. & Plickert, G. (2010). Migration and differentiation potential of stem cells in the cnidarian *Hydractinia* analysed in eGFP-transgenic animals and chimeras. *Dev Biol.* **348**, 120-9.

Layden, M.J ., Röttinger, E., Wolenski, F. S., Gilmore, T. D. & Martindale, M. Q. (2013). Microinjection of mRNA or morpholinos for reverse genetic analysis in the starlet sea anemone, *Nematostella vectensis*. *Nat Protoc.* **8**, 924-34.

Lehnert, E. M., Mouchka, M. E., Burriesci, M. S., Gallo, N. D., Schwarz, J. A. & Pringle, J. R. (2014). Extensive differences in gene expression between symbiotic and aposymbiotic cnidarians. *G3 (Bethesda)* **4**, 277-95.

Marlow, H., Roettinger, E., Boekhout, M. & Martindale, M. Q. (2012). Functional roles of Notch signaling in the cnidarian *Nematostella vectensis*. *Dev Biol.* **362**, 295-308.

Momose, T. & Houliston, E. (2007). Two oppositely localised frizzled RNAs as axis determinants in a cnidarian embryo. *PLoS Biol.* **5**, e70.

Muscatine, L. The role of symbiotic algae in carbon and energy flux in coral reefs. In *Coral Reefs* (*ed*. Zubinsky, Z.) 75-87 (Elsevier, 1990).

Renfer, E. Amon-Hassenzahl, A., Steinmetz, P. R. & Technau, U. (2010). A muscle-specific transgenic reporter line of the sea anemone, *Nematostella vectensis*. *Proc Natl Acad Sci USA* **107**, 104-8.

Riedl, J., Crevenna, A. H., Kessenbrock, K., Yu, J. H., Neukirchen, D., Bradke, F., Jenne, D., Holak, T. A., Werb, Z., Sixt, M. & Wedlich-Soldner, R. (2008). Lifeact: a versatile marker to visualize F-actin. *Nat Methods* **5**, 605-7.

Rodriguez-Lanetty, M., Wood-Charlson, E., Hollingsworth, L., Krupp, D. & Weis, V. (2006). Temporal and spatial infection dynamics indicate recognition events in the early hours of a dinoflagellate/coral symbiosis. *Mar Biol* **149**, 713-9.

Schindelin, J., Arganda-Carreras, I., Frise, E., Kaynig, V., Longair, M., Pietzsch, T., Preibisch, S., Rueden, C., Saalfeld, S., Schmid, B., *et al.* (2012). Fiji: an open-source platform for biological-image analysis. *Nat Methods* **9**, 676-82.

Sliogeryte, K., Thorpe, S. D., Wang, Z., Thompson, C. L., Gavara, N. & Knight, M. M. (2016). Differential effects of LifeAct-GFP and actin-GFP on cell mechanics assessed using micropipette aspiration. *J Biomech.* **49**, 310-7.

Sunagawa, S., Wilson, E. C., Thaler, M., Smith, M. L., Caruso, C., Pringle, J. R., Weis, V. M., Medina, M. & Schwarz, J. A. (2009). Generation and analysis of transcriptomic resources for a model system on the rise: the sea anemone *Aiptasia pallida* and its dinoflagellate endosymbiont. *BMC Genomics* **10**, 258.

Technau, U. & Steele, R. E. (2011). Evolutionary crossroads in developmental biology: Cnidaria. *Development*. **138**, 1447-58.

van Oppen, M. (2001). *In vitro* establishment of symbiosis in *Acropora millepora* planulae. *Coral Reefs* **20**, 200.

Wakefield, T. S. & Kempf, S. C. (2001). Development of host- and symbiont-specific monoclonal antibodies and confirmation of the origin of the symbiosome membrane in a cnidarian-dinoflagellate symbiosis. *Biol Bull* **200**, 127-43.

Weis, V. M., Davy, S. K., Hoegh-Guldberg, O., Rodriguez-Lanetty, M. & Pringle, J. R. (2008). Cell biology in model systems as the key to understanding corals. *Trends Ecol Evol* **23**, 369-76.

Wessel, G. M., Reich, A. M. and Klatsky, P. C. (2010). Use of sea stars to study basic reproductive processes. *Syst. Biol. Reprod. Med.* **56**, 236–45.

Wittlieb, J., Khalturin, K., Lohmann, J. U., Anton-Erxleben, F. & Bosch, T. C. (2006). Transgenic *Hydra* allow *in vivo* tracking of individual stem cells during morphogenesis. *Proc Natl Acad Sci U S A* **103**, 6208-11.

Wolfowicz, I., Baumgarten, S., Voss, P. A., Hambleton, E. A., Voolstra, C. R., Hatta, M. & Guse, A. (2016). *Aiptasia* sp. larvae as a model to reveal mechanisms of symbiont selection in cnidarians. *Sci Rep* **6**, 32366.

Xiang, T., Hambleton, E. A., DeNofrio, J. C., Pringle, J. R. & Grossman, A. R. (2013). Isolation of clonal axenic strains of the symbiotic dinoflagellate *Symbiodinium* and their growth and host specificity. *J Phycol* **49**, 447-58.

Yasuoka, Y., Shinzato, C. & Satoh, N. (2016). The mesoderm-forming gene brachyury regulates ectoderm-endoderm demarcation in the coral *Acropora digitifera*. *Curr Biol.* **26**, 2885-92.

Yellowlees, D., Rees, T. A. V. & Leggat, W. (2008). Metabolic interactions between algal symbionts and invertebrate hosts. *Plant Cell Environ.* **31**, 679-94.

Figure legends

Figure 1: Spawning induction and *in vitro* fertilization in *Aiptasia*
(**A**) Percentage of female tanks containing spawned eggs on each day of two consecutive artificial lunar cycles. Duration of the blue-light stimulus (spawning induction cue) is indicated in grey; the expected spawning period is indicated with a speckled background (total of 24 tanks). (**B**) Percentage of spawning events on each weekday (total from 24 weeks), allowing microinjection during working hours. (**C**) Female animal with egg patch nearby (arrowhead). Scale = 5 mm (**D**) Gelatin coating increases fertilization success (n=3, $p<0.01$). Error bars represent standard deviations. (**E**) Fertilization success rapidly decreases over time after spawning (n=5). Error bars represent standard deviations.

Figure 2: Microinjection of *Aiptasia* zygotes
(**A**) Microinjection dishes are prepared by affixing a strip of 80 µm nylon mesh on the bottom of a small petri dish lid using silicon grease around the edges. (**B**) Zygotes are transferred into a microinjection dish filled with FASW, where they sink to the bottom and into individual holes in the mesh. Scale = 200 µm (**C**) Microinjection set-up with stereoscope (s), fluorescence lamp (f), micromanipulator (m), injection pedal (not shown) and FemtoJet injector (i). (**D**) Co-injection of dextran-AlexaFluor 594 allows identification of zygotes that have been successfully injected. Injected zygotes are brightly fluorescent (white arrowhead), whereas uninjected zygotes appear dark (black arrowhead). Asterisk marks a 4-cell embryo. Scale = 200 µm. (**E**) The injection session proceeds until most zygotes assume a box-like shape, indicating imminent cleavage. Scale = 100 µm. (**F**) Developing embryos (arrowhead) and unfertilized eggs can be clearly differentiated 4-5 hours post-fertilization (hpf). Scale = 50 µm.

Figure 3: Microinjection of recombinant Lifeact-eGFP protein
(**A**) SDS-PAGE of recombinantly expressed and purified Lifeact-eGFP protein with an expected size of 28 kDa. (**B**) Zygotes were injected with ~3.4 mg/ml Lifeact-eGFP protein and fixed 2, 4, 6 and 24 hpf. Maximum projections of 5 z-planes near the surface or centre of the embryo are shown. Scale = 25 µm.

Figure 4: Microinjection of mRNA to fluorescently label nuclei and cell outlines
(**A**) Schematic representation of bicistronic *in vitro* transcribed *NLS-eGFP-V2A-mCherry-CaaX* mRNA: eGFP with a nuclear localization signal (NLS) is coupled to mCherry with a C-terminal CaaX box for farnesylation and insertion into the membrane. The fluorophores are separated by the self-cleaving V2A peptide. (**B**) mRNA was injected into zygotes and embryos were fixed 6 hpf and 1 and 4 days post-fertilization (dpf). Left panels show green channel with GFP-label nuclei, middle panels show red channel with mCherry-labeled membranes, and the right panel shows the merged images (nuclei, green; cell outlines, red). Scale = 25 µm. (**C**) Larvae expressing the injected *NLS-eGFP-V2A-mCherry-CaaX* mRNA and containing acquired symbiont cells (brightly autofluorescent in red channel). Symbionts within endodermal tissue (arrowhead) can be distinguished from those in the gastric cavity (asterisk). Larvae were incubated with *Symbiodinium* strain SSB01 at a concentration of 100,000 cells per ml for 3 days. Scale = 25 µm.

Figure 1

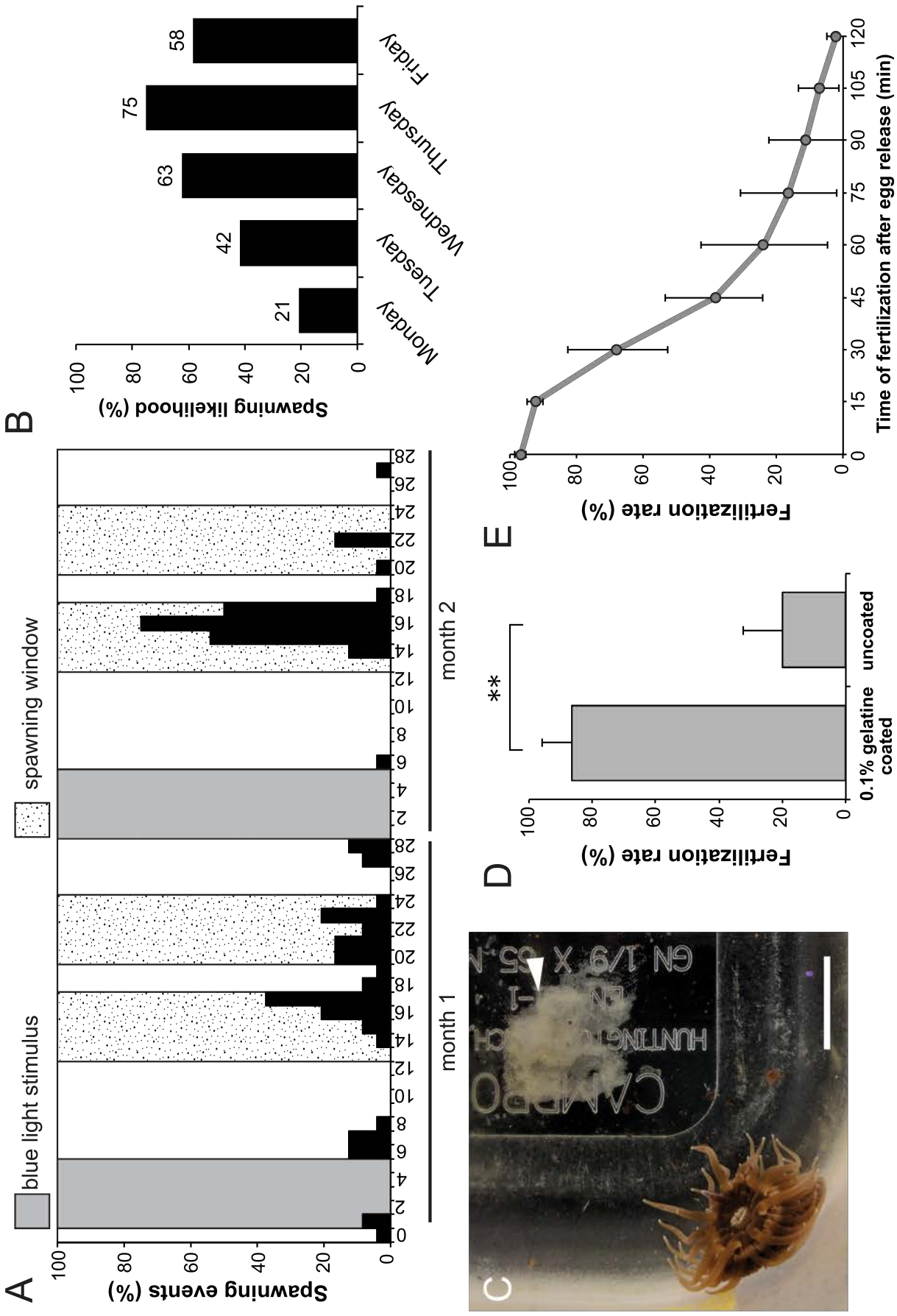

Figure 2

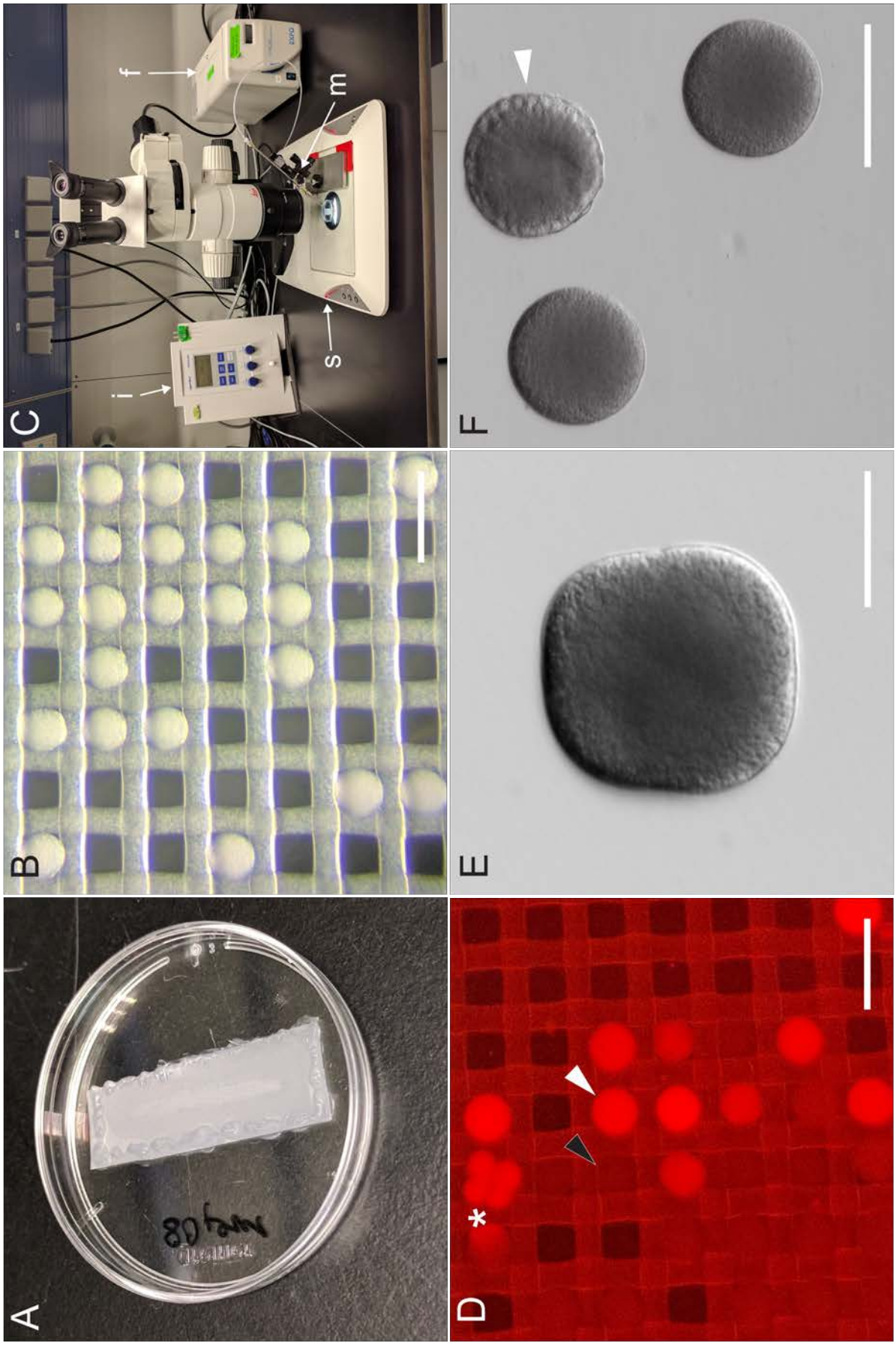

Figure 3

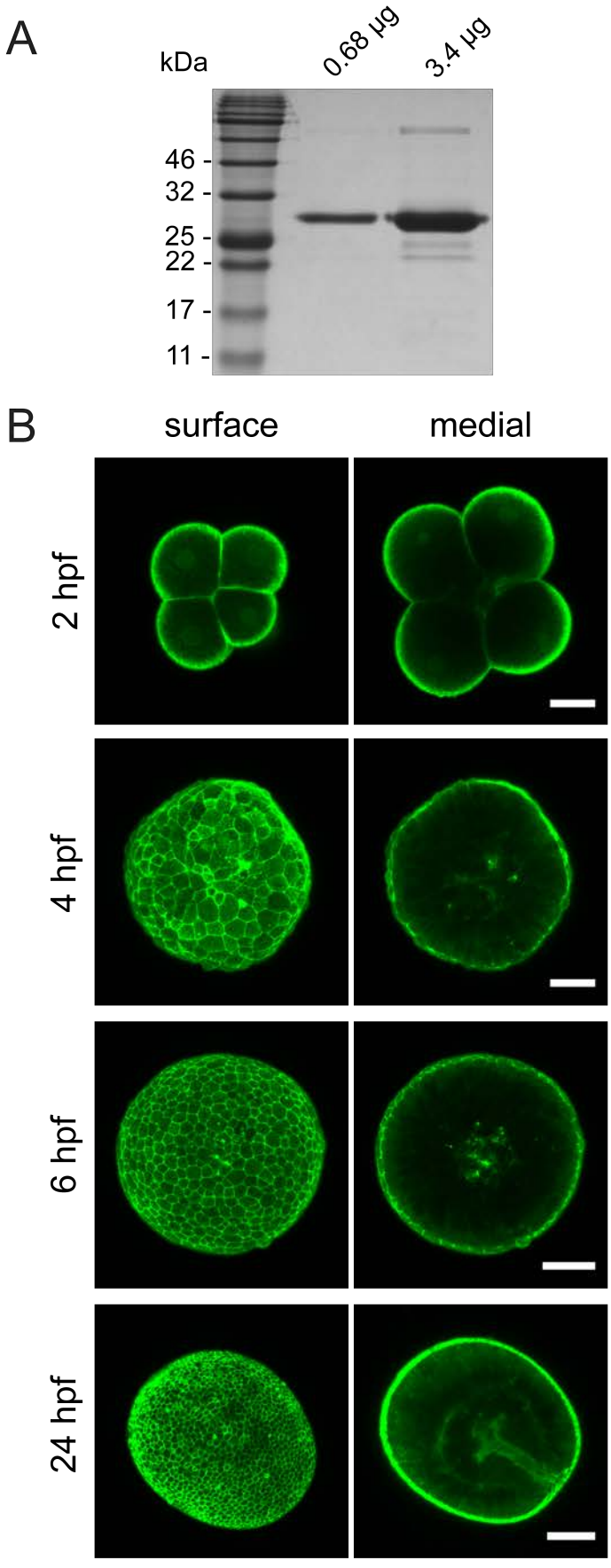

Figure 4